Nuclear Engineering and Design 418 (2024) 112908

Contents lists available at ScienceDirect

Nuclear Engineering and Design

journal homepage: www.elsevier.com/locate/nucengdes

Sensitivity analysis of simulated premixed layer and vapour explosion in stratified configuration

Janez Kokalj [a,*], Mitja Uršič [a], Matjaž Leskovar [a], Renaud Meignen [b]

[a] Jožef Stefan Institute, Jamova cesta 39, SI-1000 Ljubljana, Slovenia
[b] Institut de Radioprotection et de Sûreté Nucléaire (IRSN), Cadarache Nuclear Center, BP 3, 13115 Saint-Paul-lez-Durance, France

ARTICLE INFO

Keywords:
Nuclear safety
Severe accident
Fuel–coolant interaction
Vapour explosion in stratified configuration
Premixed layer formation
Sensitivity analysis

ABSTRACT

Experiments of fuel–coolant interaction in stratified geometry at the PULiMS and SES (KTH, Sweden) test facilities resulted in spontaneous steam explosions. Prior to the explosion, a premixed layer of ejected melt drops in the water layer was observed in the experiments. Based on the experimental and analytical knowledge, we have recently developed a model for premixed layer formation in the Fuel-Coolant Interaction code MC3D and applied it to estimate steam explosion energetics.

In the paper, a sensitivity study of this model is performed on the three main uncertain parameters of the premixed layer formation model, which define the melt fragmentation rate, the size of the ejected melt drops and the ejected melt drop velocity. The analysis is performed against the SES S1 and the PULiMS E6 experimental results. The chosen tests were selected as in both of them the same material was used, the geometry was similar, and both of them resulted in a spontaneous steam explosion. The effects can be observed in all the performed analyses and they are consistent in simulations of both experiments, affecting the premixed layer height as well as the explosion strength and duration. Some uncertainty of the experimental results is assessed, with the main limitation related to the visual observations. The combination of both analyses provides us with the assessment of future work necessity and prioritization.

The presented sensitivity analysis of the premixed layer formation model enables a more reliable assessment of the stratified vapour explosion risk and its uncertainty in nuclear power plants and other industries.

1. Introduction

In the event of a severe accident in a light-water nuclear power plant, the molten reactor core may come in contact with the coolant water (Corradini et al., 1988; Seghal, 2012; Theofanous, 1995). This interaction is commonly referred to as a fuel–coolant interaction (FCI). One of the possible consequences is a rapid transfer of the thermal energy from the molten corium to the coolant. If the time scale of the phenomenon is smaller than the characteristic time of the pressure relief of the created and expanding vapour – this is known as a vapour explosion (Berthoud, 2000; Corradini et al., 1988; Seghal, 2012; Turland and Dobson, 1996). The process can escalate as part of the released mechanical energy enhances further fine fragmentation of the melt leading to more rapid heat transfer from the melt to the coolant. Considering the amount of thermal energy in the liquid corium melt at about 3000 K, and pressure peaks in the order of 100 MPa, vapour explosion can present a credible threat to the structures, systems and components within the reactor containment building (Cizelj et al., 2006; Grishchenko et al., 2013; Leskovar and Uršič, 2009; Uršič and Leskovar, 2010). It can also present a threat to the reactor containment integrity, which would result in a radioactive material release into the environment and present a threat to the general public safety.

The significance of both in-vessel and ex-vessel vapour explosions gained recognition also from the OECD, prompting the initiation of the SERENA (Steam Explosion Resolution for Nuclear Applications) research program in 2002 (Blundell, 2015; Hong et al., 2013; Sairanen et al., 2007). The program's primary objectives were to assess the capabilities of FCI computer codes in simulating steam explosions. As part of the SERENA project, experimental tests were conducted at the TROI facility (KAERI, S. Korea) and KROTOS facility (CEA, France). Ex-vessel FCI was identified as a top-priority safety concern within the framework of the SARNET (Severe Accident Research NETwork of excellence) programme (Albiol and Haste, 2008). The primary aim of the SARNET program was to create a network of European research capabilities

* Corresponding author.
E-mail address: janez.kokalj@ijs.si (J. Kokalj).

https://doi.org/10.1016/j.nucengdes.2024.112908
Received 21 August 2023; Received in revised form 20 December 2023; Accepted 6 January 2024
Available online 13 January 2024

focused on severe accidents. Some experimental research related to steam explosions in stratified configuration was carried out as part of the SAFEST (Severe Accident Facilities for European Safety Targets) project (Miassoedov et al., 2015). However, certain aspects required further analysis, as indicated by Meignen et al., (2014b). Within the context of the French Post-Fukushima Research Program, the ICE (Interaction Corium-Eau) project, focusing on FCI, was initiated in 2014 (Meignen et al., 2017). Its objective is to address various gaps, identified in the SERENA and SARNET programmes. Currently, from 2019 to 2024, the OECD ROSAU (Reduction Of Severe Accident Uncertainties) programme is actively working to reduce the knowledge gaps and uncertainties associated with the progression of severe accident.

In nuclear safety, the vapour explosions are typically analysed in the melt jet-water pool configuration (Hong et al., 2013; Huhtiniemi et al., 1999; Leskovar et al., 2016; Seghal, 2012). The complexity of the melt breakup is caused by the hydrodynamic and thermal interactions that occur simultaneously. The hydrodynamic breakup of a liquid melt drop is usually determined based on the critical Weber number, which considers the hydrodynamic forces and the surface tension force. Only few works are available in the literature for data concerning the fragmentation of liquid drops in another liquid, which is the configuration of interest. Pilch and Erdman (Pilch and Erdman, 1987) and Gelfand (Gelfand, 1996) provided reviews and results on which the MC3D fragmentation model is verified. Concerning the low Weber numbers, several studies have reported the existence of a specific thermal fragmentation mechanism (Nelson and Duda, 1981; Nelson and Duda, 1985; Park et al., 2005). There have been several proposals to explain the phenomenon, but it is now accepted that it should come from the destabilisation of the vapour film surrounding the drops, and impacts of water jets at the drop surface, leading to high heat transfer and local pressurization, the instability of the melt surface and formation of jets and fine fragment (Lamome and Meignen, 2008; Yakush and Sivakov, 2023). In fact, the presented fragmentation model is based on a similar mechanism. Nevertheless, the drop thermal fragmentation is expected to initiate vapour explosions in some conditions. It is a good candidate for the triggering of the stratified vapour explosion as well. However, large vapour explosions are expected to be possible only through hydrodynamic phenomena, which becomes rapidly predominant when the Weber number increases. In addition, special attention in past research was given to solidification effects. The crust formation (Uršič et al., 2011) is especially important regarding the potential participation of the melt in a vapour explosion. The effect of solidification on drop fragmentation in liquid–liquid media was investigated by Haraldsson et al. (Haraldsson et al., 2001) and they proposed the criteria under which a melt drop breaks up.

However, the results from experiments performed at the PULiMS and SES facilities (KTH, Sweden) again raised interest in geometry with a continuous layer of melt under a layer of water, called stratified configuration (Grishchenko et al., 2013; Kudinov et al., 2017). In these experiments, the bubble's growth and collapse with splashes of melt were observed. This interaction of the melt with the coolant before the vapour explosion occurs is referred to as the premixed layer formation.

Based on the experimental and analytical knowledge, a model for the premixed layer formation was developed (Kokalj et al., 2021; Kokalj et al., 2023). The model was implemented as a patch into the Eulerian fuel–coolant interaction code MC3D (IRSN, France) (Meignen et al., 2014a; Meignen et al., 2014c) and validated against the SES S1 (De Malmazet et al., 2017) and the PULiMS E6 (Grishchenko et al., 2013; Konovalenko et al., 2012; Kudinov et al., 2017) experimental results. Overall, the simulation results agreed with the experimental results. However, to enable a more reliable assessment of the stratified vapour explosion risk in nuclear power plants and other industries, additional sensitivity analysis for the premixed layer formation model is performed and discussed within this paper. Namely, by knowing the model sensitivity, the confidence in the evaluation of the modelled phenomena would be significantly increased. The presented analysis is based on the SES S1 and PULiMS E6 experimental tests.

Our research aims to advance the knowledge, understanding and modelling of fuel–coolant interaction and vapour explosions in stratified configuration. The aim is to ensure that the model provides the best possible predictions for the fuel–coolant interaction in stratified configuration and to assess the effect of the model parameters on the premixed layer formation simulation.

2. Simulation of premixed layer formation and explosion

2.1. Model for premixed layer formation

The phenomenon of the premixed layer formation and subsequent vapour explosion is complex. Our previously developed model for the premixed layer formation in the area of formed stratified melt-coolant configuration (Kokalj et al., 2021) is based on the formation, growth and collapse of vapour bubbles, which seems to be the most plausible mechanism (Kokalj et al., 2019). The melt is usually hot enough for the boiling of the coolant. The bubbles condense and collapse because of the cooling of the superheated vapour (Melikhov et al., 2020). During the bubble collapse, water at the bubble interface accelerates towards the melt surface, creating a so-called coolant micro-jet. The coolant micro-jet impacts the melt surface and can produce melt surface instabilities and fragmentation of the melt.

As presented in details in (Kokalj et al., 2021; Kokalj et al., 2023) our developed model describes the premixed layer formation with three main parameters: the ejected melt drops diameter, their velocity, and the fragmentation rate. The melt drop diameter modelling considers the existence of the melt surface instabilities causing melt fragmentation. The base model equation for the melt drop diameter (d) in the premixed layer formation model (Eq. (1) is related to the most dangerous wavelength (Λ) on the surface:

$$d = C_d \cdot 0.25 \cdot \Lambda, \tag{1}$$

where factor 0.25 considers the size of the ejected melt droplet as a quarter of the most dangerous wavelength. The base model is multiplied by the tuning factor C_d to compensate for a simplified description of the reality. The fragmentation rate (Γ) is the ejected volume per unit of time and area, thus defined as the volume of the melt drop divided by the square of the most dangerous wavelength, multiplied by the frequency of melt ejections (F). In our model, the frequency is considered to be proportional to the frequency of the vapour bubble formation and collapse. As the base model equation is a simplified description of reality it is multiplied with the tuning factor C_f:

$$\Gamma = C_f \cdot \frac{\pi d^3 F}{3\Lambda^2}. \tag{2}$$

Finally, the velocity, calculated from the acoustic energy (as shown for their experiments by Caldarola and Kastenberg (1974), this is lower limit for energy) is in our model (Kokalj et al., 2021) multiplied with the tuning factor C_v:

$$v = C_v \sqrt{C_{v1} \cdot C_{v2} \cdot \frac{(p_{max} - p_0)^2 \Delta T_{sub}^2}{\Lambda^{0.8} \sqrt{\Delta p}}}, \tag{3}$$

where C_{v1} is related to the dimension of the coolant micro-jets and C_{v2} considers the liquid and melt material properties. p_0 is the ambient pressure, p_{max} is the pressure, caused by coolant micro jets that act on the melt, ΔT_{sub} is subcooling of coolant, Δp is the difference between the pressure inside and the pressure outside of the bubble.

2.2. Modelling with MC3D

The validation of our model was done by comparing the computational simulations with the experimental results (Kokalj et al., 2021).

The developed model was implemented as a patch in the MC3D computational fluid dynamic code V3.9.0.p1. MC3D is being developed at IRSN (France), specifically for the simulations of fuel–coolant interactions. MC3D is suitable for our research because it covers both phases of the vapour explosion - the premixing phase as well as the explosion phase. The premixing phase module (Meignen et al., 2014a) covers the initial mixing of the melt and the coolant and this module was upgraded with the premixed layer formation model, developed in the frame of our research work. In case a vapour explosion occurs, the results from the premixing phase module serve as an input for the explosion phase module. The explosion phase module (Meignen et al., 2014c) concerns the fine fragmentation of the melt during the explosion and the heat transfer between the created fine fragments and the coolant.

MC3D uses an Eulerian description, wherein continuity equations for energy, momentum, and mass are solved separately for each phase (liquid and vapour coolant, melt drops, continuous melt, and non-condensable gases). Numerically, the phases are represented by volume, velocity and temperature fields. For simulating the premixed layer and the consequent vapour explosion, the most important heat transfer contribution is from the melt drops to the liquid coolant. The default heat transfer modelling in the MC3D code for melt drop film boiling is obtained by the Epstein-Hauser correlation for the forced convection, which is the most common regime (Meignen et al., 2014a).

Primary fragmentation is represented as a transfer of mass from the continuous melt field to discrete melt drop fields. It is not feasible to represent the trajectories of the melt drops with a single Eulerian field since they are typically ejected upward and then fall downward, resulting in different velocity directions. Nevertheless, the melt drops can be effectively portrayed using the MUlti-DROP model, in which distinct melt drop volume fields are characterized by specific diameters (utilizing the MUSIG method). While any number of fields can be employed, they must be consolidated into one or two velocity fields at most to accurately describe the movement of melt drops both upward and downward.

In the standard model of MC3D, mass transfer between the drop fields is governed by the secondary fragmentation model, which involves the breakdown of large drops into smaller ones. Both the premixing and explosion models adhere to the same principles. However, in the explosion model, the continuous melt field is not utilized. Instead, an additional field is employed to represent the small fragments resulting from fine fragmentation within the drop field during the explosion.

The vertical ejection and subsequent gravitational fall of the drops cannot be easily represented with an Eulerian approach since it is necessary to discriminate the newly fragmented hot drops going up and those, more or less cooled, going down back in the continuous layer. In the present model, a two-melt-drop-group approach is applied. This approach employs two volume fields, each with its corresponding velocity and temperature fields. In the implemented patch of the MC3D code, this model is adapted such that one group is designated for upward-moving drops (with positive velocity), and another group is designated for descending drops (with negative velocity). The group of upward-moving drops is fed by the continuous melt fragmentation at the specified fragmentation rate, drop size, and initial drop velocities as defined in Section 2.1. The second group is fed from the first group through a modification of the mass transfer law, which occurs in the cells corresponding to the velocity of the first group drops becoming negative.

In the premixing phase simulations, the input parameters include the material properties of the melt, initial conditions (melt, water, and gas temperature), and the initial geometry. The melt pouring and spreading are not modelled. Therefore, initially, all the continuous melt is described as a melt pool with a diameter assessed from the experiment, whereas the height is calculated from the released mass of melt. For the premixing phase of the calculation, the melt is enclosed at the side with plates. The objective of the side plates is to keep the melt pool size constant.

For the explosion phase simulations, the results obtained from the premixing phase serve as input data. The plates, enclosing the melt pool are removed to prevent possible pressure shock wave reflections. The explosion is triggered by the defined trigger (location, composition, pressure). The explosion modelling has not been modified.

2.3. Scope of analyses

Two experimental tests of fuel–coolant interaction in stratified configuration, PULiMS E6 and SES S1 are simulated The analyses of PULiMS E6 and SES experimental cases are based on the previously analysed best estimate (BE) simulations (Kokalj et al., 2021). In the BE analysis, the simulated force signals on the bottom of the domain and total gained impulses were compared with the experimental results. For the presented results, the trigger contributions to the force on the bottom and to the impulse were deducted. The force signal was calculated as the differential force compared to the initial state.

The BE simulation results are congruent with the experimental results and more details can be found in (Kokalj et al., 2021). The simulations adequately calculate the premixed layer observed in the experiment. For the explosion phase, the simulations more accurately describe the initial period. The calculated force and the impulse are in good agreement with the experiments, but later, the explosion strength is underestimated. The underestimation is much smaller for the SES S1 experiment than for the PULiMS E6 experiment. A possible explanation was given related to the amount of melt, participating in the explosion. This possible underestimation in the mass of melt drops in our simulations could be related to considering only the bubble formation, growth and collapse mechanism for the premixed layer formation. The experimental phenomena are complex and it would be expected, that some amount of mixing between the melt and the water could be a consequence of other possible mechanisms, e.g. jet breakup, water entrapment under the melt, and mixing during the explosion itself. Indeed, the jet breakup contribution in the PULiMS E6 experiment with the free jet penetration through 20 cm of water prior to reaching the test section bottom must be larger than for the SES S1 experiment with the free jet penetration through 2.5 cm of water.

To improve the understanding of the modelled phenomena, the effects of the model's main three parameters (see Section 2.1) are analysed in detail within this paper. The three parameters are being varied independently in the analysis. This way, their individual effect on the simulations can be assessed, while it should be pointed out that considering the overall phenomenon the parameters affect each other, e.g. considering the same energy of the instabilities, the larger melt drops would result in smaller initial melt drop velocity and larger fragmentation rate. Considering the uncertainty with which we assessed the individual parameters from the experimental results, contrary to the highly complex and intertwined combined phenomenon, this way at least some idea on the uncertainty of the model and consequent simulations can be gained. The simulations are divided into the premixing phase and the explosion phase. The same computational model as for the BE simulations is applied (Kokalj et al., 2021).

3. Analysis of size of ejected melt drops

A sensitivity analysis is first made regarding the size of melt drops (varying factor C_d in Eq. (1)) in the premixed layer. The direct comparison of the model for the premixed layer formation with the experiments is limited to visual observations (Fig. 1). For conditions in the PULiMS and SES experiments, the typical melt drop size with our model (with the factor C_d being 1) is around 7 mm (Kokalj, 2021). This agrees with the experimental observations, but there are large uncertainties in the analysis of the experimental data, indicating also a possibility that the premixed layer consists of a whole spectrum of melt drop diameters. The BE C_d factor 1.25 (melt drop diameter of around 8.5 mm) presents also close a match with the experimental observations. Thus, the C_d

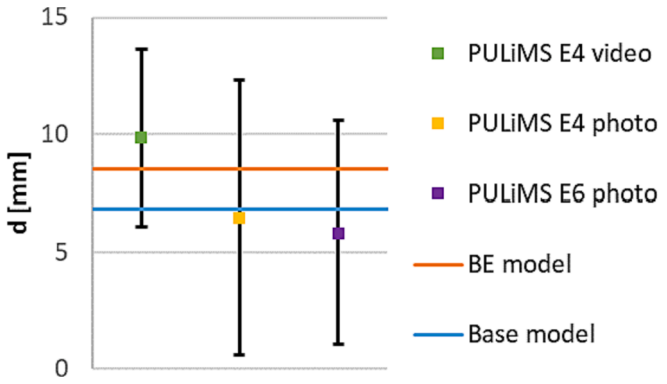

Fig. 1. Comparison of melt drop diameter with base model and model with BE value C_d = 1.25 (around 8.5 mm) and a few experimental estimations. A snapshot from the video recording, representing the melt drops formation phenomenon, and photos during the experimental tests (all KTH, Sweden) were studied. The observed typical size of the melt drops in the experiments is presented, with the estimated size spectrum shown with error bars.

factor is varied (1, 1.25 and 1.5) around the BE value 1.25.

The simulated premixed layers with different melt drop diameters for the SES S1 case can be seen in Fig. 2. The premixing phase lasted for 0.6 s, the same as in the experiment. The general pictures for all the different melt drop diameters are comparable. The larger melt drops because of smaller drag per unit mass reach a slightly larger height and the premixed layer is slightly less rich (smaller volume fraction of melt drops in the premixed layer), the total mass of melt drops in the premixed layer being similar. However, the size of melt drops affects the heat transfer and the consequent vaporization. With the smaller melt drop diameter and the same amount of melt, the total melt surface is increased and more steam is generated (right in Fig. 2). In all cases, the amount of steam in the premixture is always very small, probably due to the rather large drop diameter (compared to FCI cases with jets penetrating water pool) and short premixing time. The premixture is then essentially composed of a few percent of melt drops in water.

The sensitivity of the calculated premixed layer on the melt drop

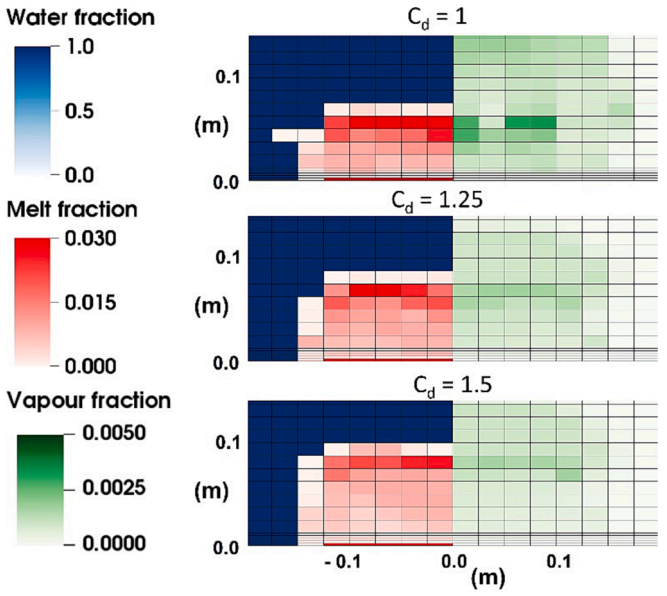

Fig. 2. Comparison of the premixed layers at 0.6 s for different melt drop diameters for SES S1 simulations on the left. The melt volume fraction is shown where its volume fraction is larger than 0.001. Everywhere else, water volume fraction is shown. The steam fraction is shown on the right. Only the side view of the central part of the simulation domain with melt is depicted.

diameter can be additionally assessed indirectly by its influence on the steam explosion. Results from the premixing phase, calculated with our model, serve then as an input for the simulation of the explosion phase. The explosions in simulations are triggered by prescribing a high pressure in one of the cells in the simulation domain at half the distance between the centre and the edge of the premixed layer. Such simulations are less prone to symmetric pressure pulse reflections (Kokalj et al., 2021) and the experimental results also indicate the non-central triggering of the explosion to be more plausible.

In Fig. 3, a comparison of the force and the total gained impulse for different melt drop diameters for the SES S1 case are shown. The force signal and the impulse are similar for the larger two melt drop diameters (C_d factors 1.25 and 1.5). The similar strength of the explosion for the larger two melt drop diameters can be explained by the similar mass of the melt drops (0.37 kg and 0.34 kg for the C_d factors 1.25 and 1.5, respectively). The maximum force for the $C_d = 1.5$ case is slightly lower compared to the $C_d = 1.25$ case, but the duration is slightly prolonged. The duration is calculated as the total impulse divided by half of the maximum force. The explosion duration can be more easily observed in Fig. 4 and on the graph of the gained impulse (left in Fig. 3). It could be explained by the longer and slower fine fragmentation of the larger melt drops. The fine fragmentation rate is in the code simulated to be inversely proportional to the melt drop diameter. This would slow down the heat transfer and consequently produce a lower and wider force signal. The time development of the medium melt drop diameter impulse is most similar to the experimental one. The initial impulse gain is almost identical to the experimental one and the duration seems to be similar.

The case with the smallest melt drop diameter (C_d factor 1) has a similar mass of melt drops (0.38 kg). However, there is no explosion in this case (Fig. 3) although the melt drops in the premixed layer are still liquid and consequently all the melt drops could participate in the explosion. It might be related to the larger volume fraction of steam because of smaller melt drops, which is damping or making it more difficult to trigger the explosion. However, this hypothesis should be further investigated, as the overall steam volume fraction inside the premixed layer in all three SES cases is below one percent (Fig. 2).

In Fig. 5, the same comparison of the force and the total gained impulse for different drop diameters is shown for the PULiMS E6 case. At this point, we should remember the simplification made earlier regarding omitting the simulation of melt pouring and spreading. In the simulations, from the beginning of premixing, the final radius of the melt pool is prescribed. This simplification overestimates the heat transfer from the melt to the water because of the larger premixed layer from the beginning of the premixing phase. As from the analysis of the mass of melt drops, no significant time dependency is observed in the simulations (Kokalj, 2021), the premixed simulation time before triggering the explosion for the PULiMS E6 test is set as 3.5 s or around half of the experimental one. This assumption regarding the triggering time seems to give a more accurate assessment of the heat transfer (heating of water and cooling of melt) while not making a larger error regarding the mass of melt drops. Compared to the SES S1 case, in the PULiMS E6 case, this contribution is more significant and, in the SES S1 case, the quasi-stationary conditions are not yet reached after half of the premixing time, therefore this correction of the triggering time is considered only in the PULiMS E6 case.

The total gained impulse does not differ significantly for different melt drop diameters. Similarly to the SES S1 case, the mass of melt drops is almost insensible to the drop diameter in the varied cases (0.61 kg for the C_d factors 1 and 1.25 and 0.60 kg for the C_d factor 1.5, respectively). Although the explosion is much stronger than in the SES S1 calculations (a factor of 3), the impulse remains largely below the experimental measured and larger discrepancies between the simulation and experimental results can be observed. However, as stressed before (Kokalj et al., 2021), besides the bubble formation, growth and collapse, other mechanisms, relevant to the individual experimental geometry (e.g. jet

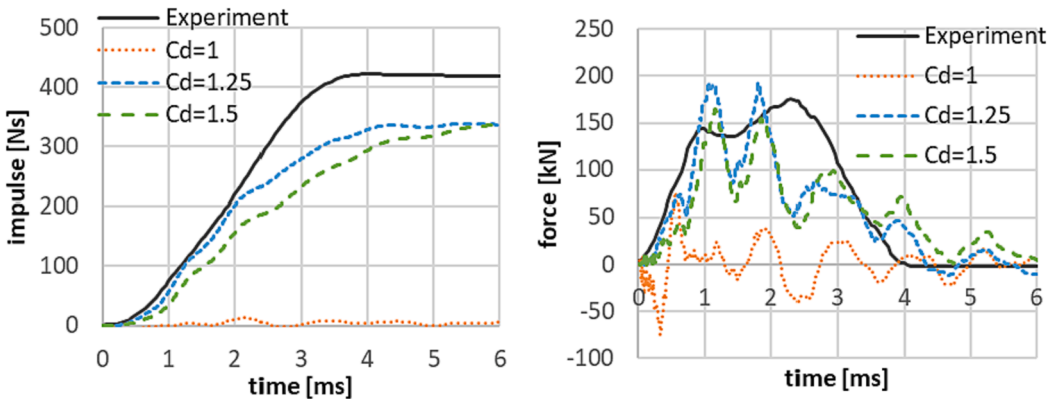

Fig. 3. Comparison of the force and total gained impulse on the bottom plate for the SES S1 case for different melt drop diameter factors C_d.

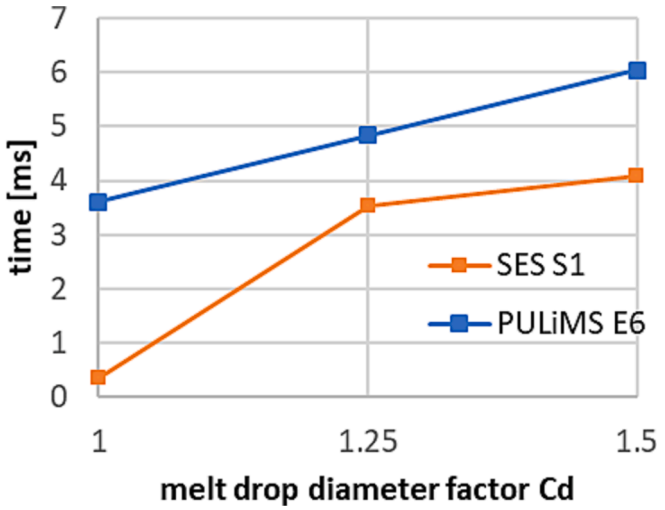

Fig. 4. Duration of the explosion for the individual simulation cases regarding the melt drop diameter factors C_d. Interpolation lines are added for easier observation of the trend.

break-up), could serve as additional sources of the melt instabilities, contributing to the explosion strength. Additionally, a contribution to the amount of the melt-coolant mixture, which could participate in the vapour explosion, can be a consequence of the mixing during the explosion itself. On the other hand, the force signal is significantly affected by different melt drop diameters – the maximal force almost for factor 2. The trend of the larger melt drops producing longer explosions with lower maximum force, observed in the SES S1 simulations case, is confirmed by the PULiMS E6 simulation cases (Fig. 3 and Fig. 4).

The initial force signal of the medium melt drop diameter (C_d factor 1.25) is also most similar to the experimental one. Consequently, the initial impulse gain - the explosion development for the medium melt drop diameter is almost identical to the experimental one, similar to the conclusions from the SES S1 case.

For the PULiMS E6 case, the smallest melt drop diameter does produce a strong explosion, which is not observed for the SES S1 case. Consistent with the earlier analysis, which established that larger melt drops result in longer explosions, the case involving the smallest melt drop diameter produces the shortest steam explosion with the highest force peak. Furthermore, the force signal for this case tends to overestimate the progression of the explosion. This suggests a more rapid fine fragmentation of the melt drops during the explosion, which accelerates heat transfer and, in turn, generates a force signal that is both higher and narrower. The vapour volume fraction is small (up to 1 %) also for the PULiMS E6 case, which has a longer premixing phase.

To summarize, the sensitivity analysis showed that the ejected melt drop size – factors C_d (for the same ejected melt mass) has a small effect on the explosion impulse if the steam explosion develops. On the other hand, the explosion force (or pressure) peak and the duration of the explosion are more sensitive to the ejected melt drop size, as they are related to the fine fragmentation process. Smaller melt drops produce larger maximum force and shorter explosion.

While the uncertainty of the observed melt drops diameter is relatively large, the model is moderately sensitive for simulating the steam explosion force (and pressure) and practically not sensitive for the total gained impulse of the explosions, if the explosion is triggered. It should be noted that large total impulses are more problematic for the systems,

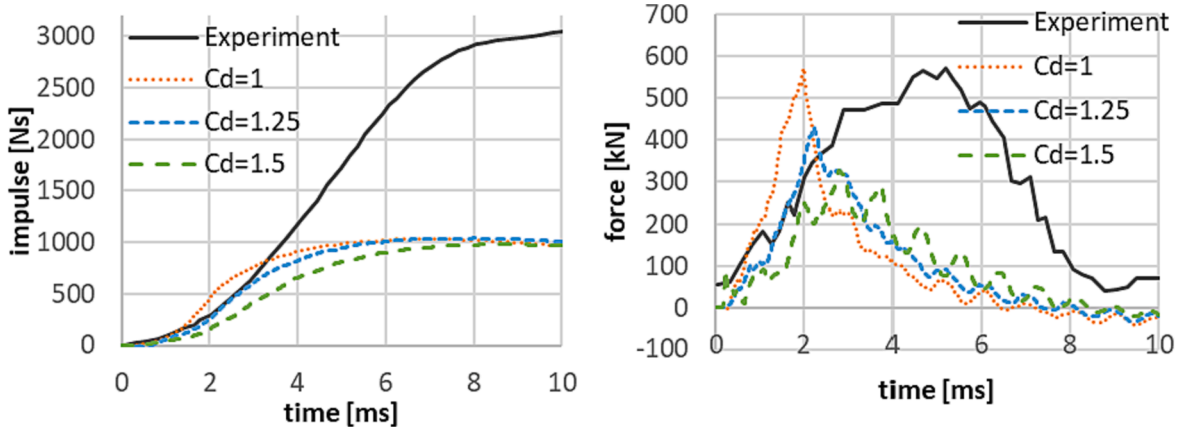

Fig. 5. Comparison of the force and total gained impulse on the bottom plate for PULiMS E6 case for different melt drop diameter factors C_d.

structures and components compared to the short pressure peaks. Therefore, while the modelling can be improved especially with advanced experimental observations and possible modelling of the melt drops diameter spectrum, the current modelling capabilities might present already a relatively good enough approximation in regard to the nuclear safety.

4. Analysis of melt fragmentation rate

The fragmentation rate is difficult to be assessed from the experiments and therefore there is, consequently, a large uncertainty. Direct comparison from the visual observation of the experiments is almost impossible. It can be assessed partially via a few parameters – the frequency of melt ejections, the melt drops diameter and the spatial distribution of melt ejections (Kokalj, 2021). The frequency of the melt ejections can be indirectly assessed from the melt drop lifetime. In Fig. 6, the experimentally observed frequency with its uncertainty is compared to the base model value, directly calculated as described in (Berenson, 1961) and the model value for frequency, considering the BE factor $C_f =$ 0.5. This BE frequency value agrees with the experimental observations if it is assumed that in Eq. (2) the melt drop diameter (d) and the most dangerous wavelength (Λ) are exactly known and that the tuning factor C_f affects only the frequency. But there are large uncertainties in the analysis of the experimental data and thus the uncertainty of the variables in Eq. (2) is large. The spatial distribution defining the most dangerous wavelength can be assessed from the distance between the individual melt ejections, however, the depth perception is difficult, also because of the smoke and the bubbles. The uncertainty of the melt drop diameter was assessed in the previous section. The product of all these uncertainties is significant while simultaneously other mechanisms (e.g. jet break-up and mixing during the explosion itself) could also contribute to the melt-coolant mixing.

The sensitivity analysis is performed with fragmentation rates multiplied by factors C_f in Eq. (2) from 0.25 up to 2, with the BE value 0.5 (Kokalj et al., 2021). The simulated premixed layers with different fragmentation rates can be seen in Fig. 7. The general pictures for lower fragmentation rates are similar for both experimental cases. As expected, the larger fragmentation rate produces a richer premixed layer (larger volume of melt drops in the premixed layer). The premixed layer is however different for the largest fragmentation rate. This is due to the fact that in some areas, the melt pool has been totally fragmented. This also affects the total mass of melt drops in the premixed layer, as seen in Fig. 8. A direct comparison with the experimental results is difficult, as during the experiment, the amount of melt drops was not determined. They fragment and coalesce back to melt and at the explosion, melt fragments were also ejected from the test section.

The sensitivity on the calculated premixed layer of the melt fragmentation rate can be assessed indirectly by its influence on the steam explosion simulations. From the previous analysis (Leskovar et al., 2019), a correlation between the melt drop volume fraction in the premixed layer and the impulse was observed. For the SES S1 case, it can be observed in Fig. 9 and Fig. 10, that the highest total impulse is gained in the $C_f = 0.5$ case. For the $C_f = 0.25$ case, the impulse is about half of the impulse for the $C_f = 0.5$ case, as expected because of the about half smaller mass of melt drops in the premixed layer. However, the impulse is significantly lower again for the $C_f = 1$ case, and again raises with larger fragmentation rates ($C_f = 2$).

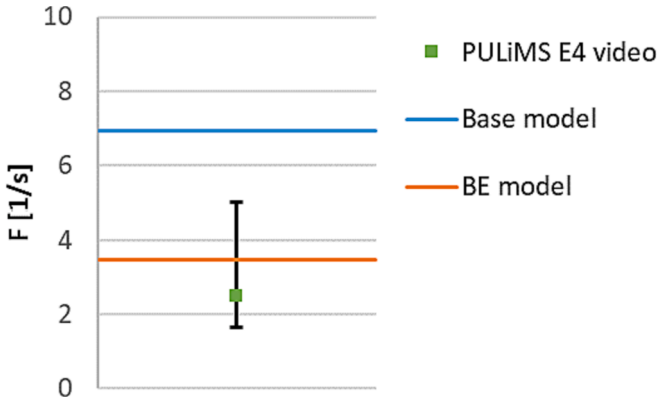

Fig. 6. Comparison of frequency of the melt ejections for the base model, the frequency in the model assuming that the BE factor $C_f = 0.5$ affects only the frequency, and the experimental estimation.

From the force signal graph, a transition in regimes can also be observed. For the lower fragmentation rates ($C_f = 0.25$ and 0.5), the force signal is lower, but more prolonged, in duration similar to the experiment. For higher fragmentation rates ($C_f = 1$ and 2), the force signal has a more pronounced first peak and then the signal decreases much earlier compared to the other two simulation cases and the experiment. It indicates that the majority of the melt drops undergo fine fragmentation during the first travelling pressure wave, while in other cases, some fine fragmentation occurs during the next few pressure reflections.

For the PULiMS E6 case, the premixed layers show a similar trend as for the SES S1 case. Because the melt pool is deeper in the PULiMS E6 case, even for the largest fragmentation rate, the melt pool area remains the same throughout the whole premixing phase. Same as in the SES S1 case, it can be observed in Fig. 10 and Fig. 11 that the impulse for the $C_f = 0.25$ is about half of the impulse for the $C_f = 0.5$ case, as expected because of the about half smaller mass of melt drops in the premixed layer. For the $C_f = 0.5$, 1 and 2 cases, the impulse is very similar, in all cases around one-third of the experimental ones.

However, the trend of the force signal in the sensitivity analysis of the fragmentation rate is clearer and more significant (Fig. 10, Fig. 11). Small factor C_f results in a small maximal force, but a more prolonged force signal. Contrary, large C_f results in a short peak of force signal with high maximal force. This would mean that a richer premixed layer (larger volume fraction of melt drops) results in quicker and more effective propagation of the fine fragmentation of the melt drops in the premixed layer.

Overall, the $C_f = 0.5$ case seems to be the most appropriate choice for the PULiMS E6 case, the same as for the SES S1 case. The initial force signal is very similar to the experimental one but then diminishes earlier. However, with a larger fragmentation rate no significant increase in the impulse can be achieved and the duration of the explosion is decreased.

To summarize, in both simulated tests the sensitivity analysis shows two regimes of the fragmentation rate effect on the total gained impulse. While in the first regime the impulse is increasing at smaller fragmentation rates, in the second regime with larger fragmentation rates it decreases or reaches a sort of plateau, where the effect is limited. On the other side, the effect on the force is more noticeable and consistent and the maximal force seems to be quite proportional to the fragmentation rate.

With the large effects of the fragmentation rate and the mass of melt in premixed layer in general on the consequent steam explosion, it seems important to reduce the uncertainty of the fragmentation rate. Only additional improved experimental observations could enable the possibility for more detailed modelling, which would provide us with a more precise estimation of the steam explosion impulse and maximal force or pressure. As mentioned, large total impulses are more problematic for the systems, structures and components compared to the short pressure peaks. In combination with the observed maximum of gained impulses and its plateau or decrease above the certain fragmentation rate this would provide us with an advantage of reducing the range of initial and boundary conditions needed for the conservative assessment of plausible steam explosions.

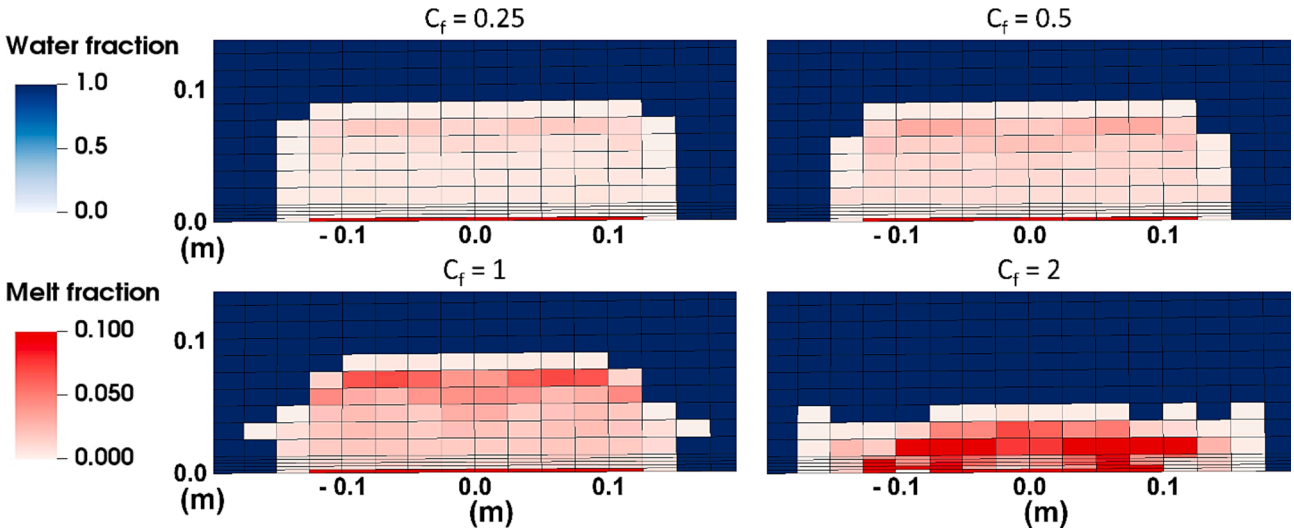

Fig. 7. Comparison of the premixed layers at 0.6 s for different melt fragmentation rates for SES S1 simulations. The melt volume fraction is shown where its volume fraction is larger than 0.001. Everywhere else, the water volume fraction is shown. Only a side view of the central part of the simulation domain with melt is depicted.

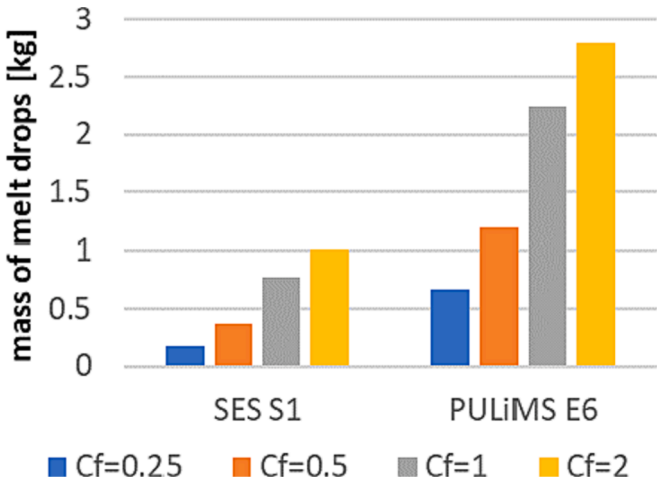

Fig. 8. Comparison of the mass of melt drops at the end of the premixing phase for different melt fragmentation rates – factors C_f for the SES S1 and PULiMS case.

5. Analysis of ejected melt drop initial velocity

Some effects of the different melt drops ejection velocity factor C_v in Eq. (3) were partially investigated in (Kokalj et al., 2021) and are here summarized to provide completeness to the reader. While the factors for the melt drop diameter and the fragmentation rate are in the order of unity, varying around the base model value, the BE tuning factor for velocity is $C_v = 6$. The velocity in the model is bounded by the upper and the lower limit based on different modelling approaches, with the ratio between them around 10 for the conditions used in the analysis. The reason for the relatively large tuning factor C_v is that for the base model the lower limit – the acoustic potential energy modelling approach was taken (Eq. (3)). Therefore, multiplying the lower limit of the velocity by a factor of 6 presents almost the average value between both limits and values of 3 and 9 present a variation of about 50 %. In Fig. 12, the BE model value can be observed compared to the model limits and both varied model cases. The model for melt drop ejection velocity is dependent on the coolant subcooling, with both analysed cases having an initial subcooling of 25 K.

The sensitivity analysis shows that the effect of different melt drops ejection velocities is pronounced already for the premixing phase. The formed premixed layer for the SES S1 case at the time of explosion triggering is shown in Fig. 13. With the increased melt drops ejection velocity, the premixed layer is higher.

An increased velocity affects also the distribution of the melt drops

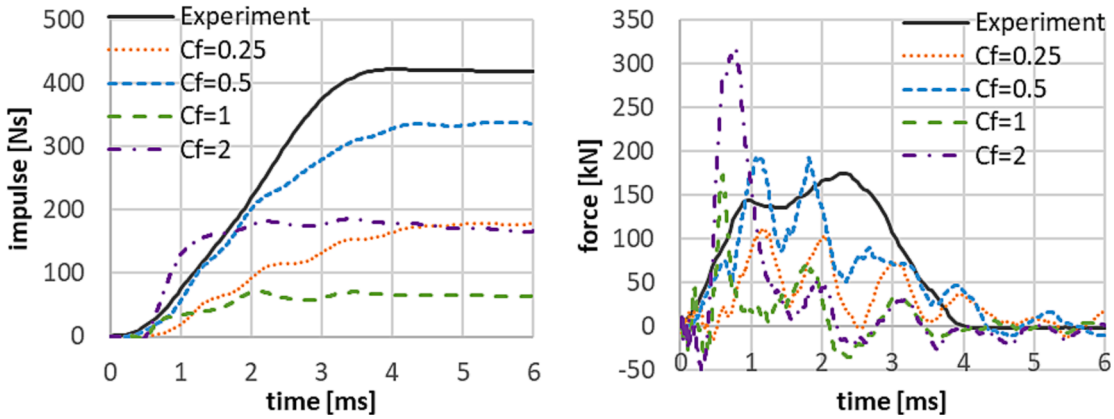

Fig. 9. Comparison of the force and total gained impulse on the bottom plate for SES S1 case for different fragmentation rate factors C_f.

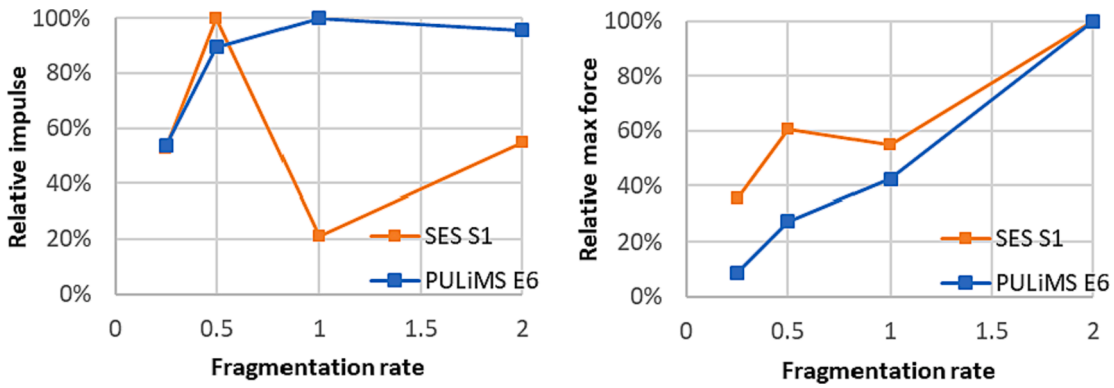

Fig. 10. Relative maximal impulse, left, and relative maximal force, right, for the individual simulation cases regarding the fragmentation rate.

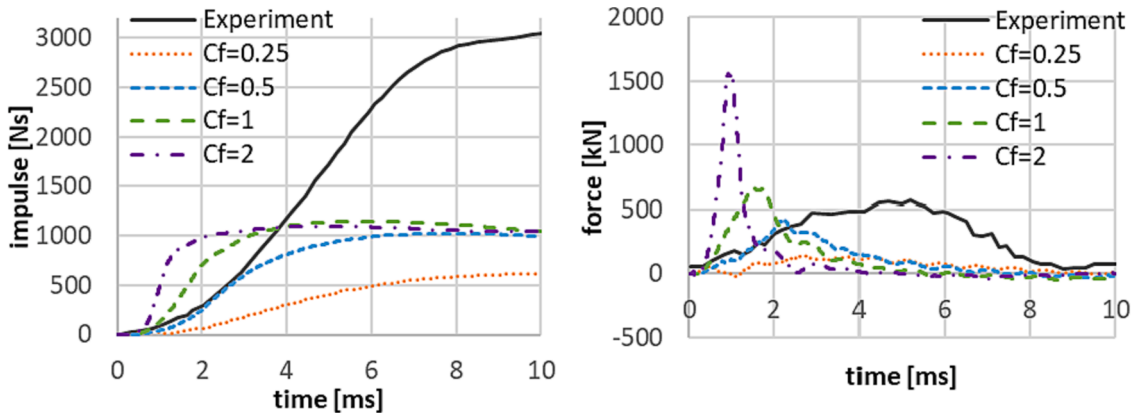

Fig. 11. Comparison of the force and total gained impulse on the bottom plate for PULiMS E6 case for different fragmentation rate factors C_f.

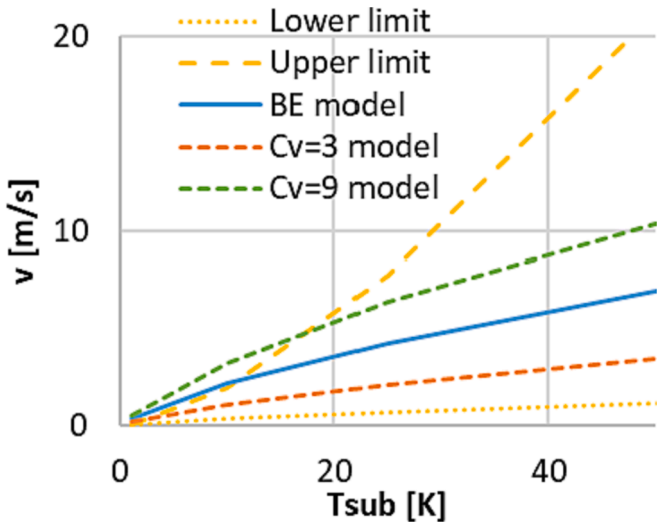

Fig. 12. Comparing the BE model value ($C_v = 6$) for ejection melt drop velocity with the model limits and the investigated varied factors $C_v = 3$ and $C_v = 9$.

(Kokalj et al., 2021). With increased velocity, the melt-drops-rich part is higher above the melt pool. In the premixed layer of the $C_v = 3$ case, the total amount of melt drops is lower because of the smaller total volume of the premixed layer, not enabling as strong explosion as in the other two cases (Fig. 14). However, despite the larger mass of melt drops due to the larger total volume of the premixed layer in the $C_v = 9$ case compared to the $C_v = 6$ case, the explosion development is similar. The $C_v = 9$ case results in only a slightly prolonged and stronger explosion, which indicates that not only the mass of the melt drops but also the composition of the melt and water mixture is of high importance for the steam explosion development.

Given the inherent uncertainty in simulating vapour explosions, the simulation results appear to be in reasonably close agreement with the experimental observations when the factor $C_v = 6$.

A sensitivity analysis on the factor C_v is also performed on the PULiMS E6 test. In Fig. 15, premixed layers for different C_v are shown at time 7 s, at which approximately the explosion occurred. There is a clear correlation between the factor C_v and the average height of the premixed layer, with the trend showing an increase in height in line with the C_v factor. Notably, the premixed layer height in the first case appears to be visually similar to the experimental observations, where melt ejections of approximately 10 cm were documented. In general, the premixed layers in the PULiMS E6 simulations, compared to the SES S1 simulations with the same factor C_v, are higher. In the case of $C_v = 6$, the average premixed layer height in the is similar to the experimental observations, however, some ejections reach up to 15 cm high. A longer premixing phase enables some convection of water to be established. It brings the cold water, as shown in Fig. 16, towards the centre of the melt pool, which results locally in higher melt ejections, as evidenced by the presence of two peaks of melt drops around 10 cm from the centre (as seen in Fig. 16). After approximately 3.5 s, the vortices in the water weaken and move outwards. The water ingression reaches only the outermost cells, leading to higher melt ejections at the sides of the melt pool. These side ejections are not observed in the SES S1 case, as the premixing duration is insufficient to establish water convection. It is unlikely to observe such well-defined water vortices in the experiments as well, as the phenomena there are much more chaotic. The melt there is spreading in waves, rapidly changing the boundary conditions for possible strong and clear natural convection vortices development.

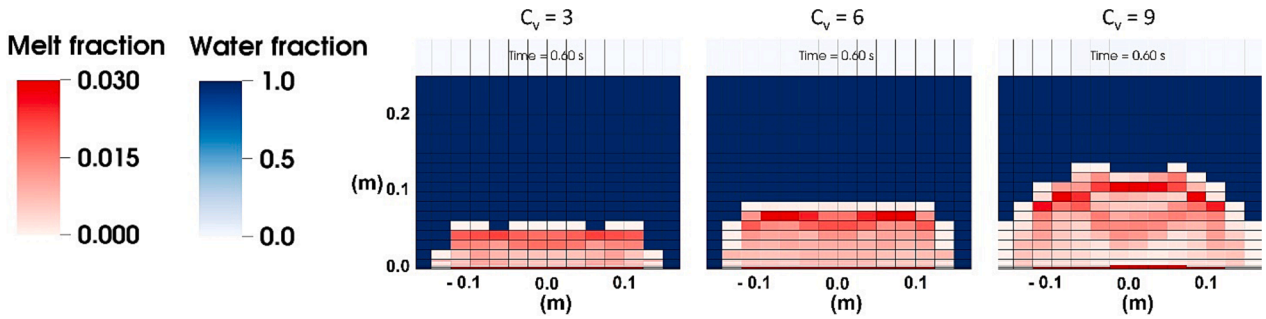

Fig. 13. Comparison of the premixed layers at time of explosion triggering for different melt drops ejection velocity factors C_v for the SES S1 simulations. The melt volume fraction is shown where its volume fraction is larger than 0.001. Everywhere else, the water volume fraction is shown. Only a side view of the central part of the simulation domain with melt is depicted.

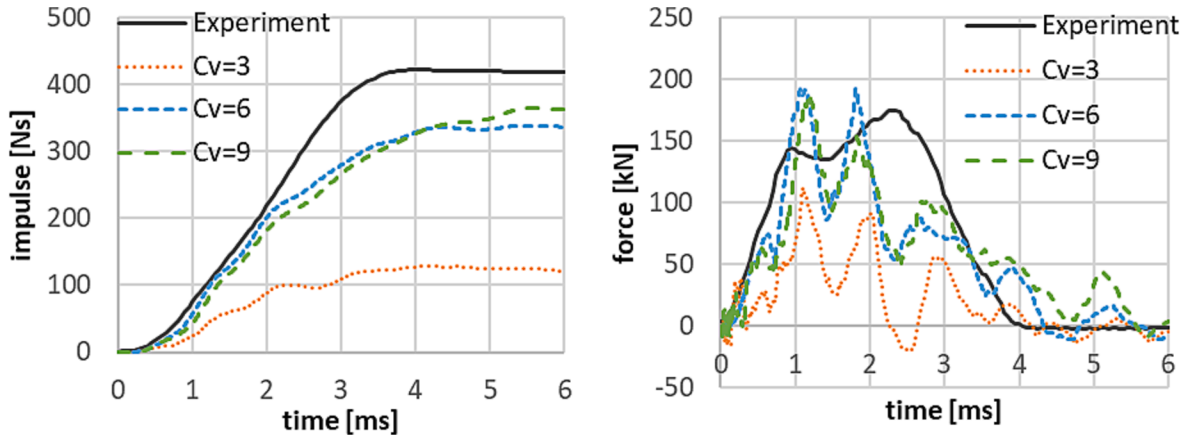

Fig. 14. Comparison of the force and total gained impulse on the bottom plate for different melt drops ejection velocity factors C_v for SES S1 simulations and experiment (figure adopted from (Kokalj et al., 2021)).

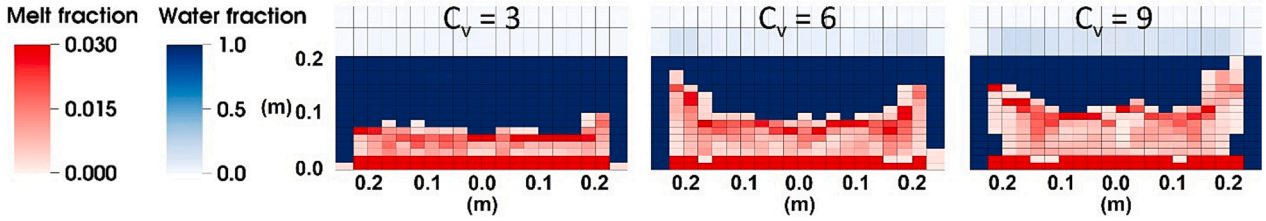

Fig. 15. Comparison of the premixed layers at 7 s for various melt drops ejection velocity factors C_v in the PULiMS E6 simulations. The melt volume fraction is shown where its volume fraction is larger than 0.001. Everywhere else, the water volume fraction is shown. The visual representation focuses on a side view of the central portion of the simulation domain with melt.

The average melt drop volume fraction in the $C_v = 3$ case is around 2 % and around 1.5 % in the other two cases, which seems to be in agreement with the experimental results (Kokalj, 2021). Due to the longer premixing phase, the steam volume fraction in the premixed layer is at the time of the triggering approximately twice as in the SES S1 cases, but still under 1 %.

For PULiMS E6 the analysis of the different melt drops ejection velocity factors C_v (Eq. (3)) effect is further extended to the explosion phase. Like the SES S1 case, the intensity of the explosion rises with the increased C_v factor (as indicated in Fig. 17). This is primarily due to the larger premixed layer resulting from higher C_v values. However, it's worth noting that in all the computed scenarios, the overall gained impulse from the explosion is consistently underestimated.

It seems that the code accurately simulates the initial phase of the steam explosion in the aspects of force and impulse. However, the explosion strength of the second part is being underestimated. Overall, opting for the factor C_v of 6 in the simulations appears to be a reasonable choice also for the PULiMS E6 experiment, although it may not capture the explosion phenomena as good as it does for the SES S1 case.

To summarize, the sensitivity analysis of the melt drops ejection velocity in general shows that the effect on the premixed layer height is large enough to be easily visually observed. However, the effect on the explosion is less significant, a 50 % change in the model's velocity from the BE parameter in most of the cases only slightly increases the maximal force and the total gained impulse. The duration of the explosion is also not affected.

The melt drops ejection velocity can be compared indirectly by the maximal height of the premixed layer, based on the visual observation of the experimental results. Considering the large effect on the simulated premixed layer height, the melt drops ejection velocity can be assessed most easily from the all three discussed model parameters, also probably with the smallest uncertainty. Therefore, it seems that the melt drops

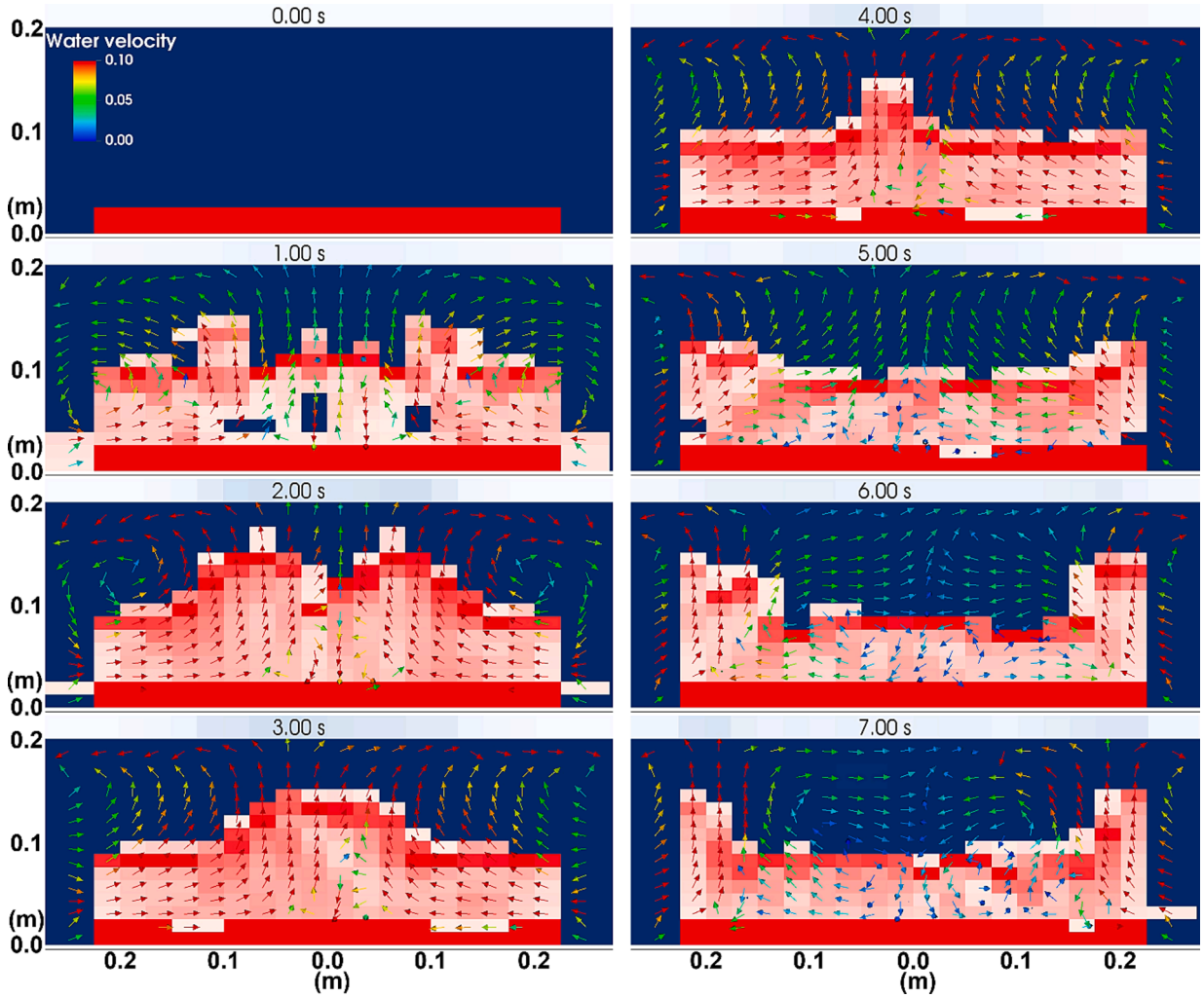

Fig. 16. Water velocity in the cells in the symmetry line (vectors show direction, colour of vectors shows velocity magnitude, scale in m/s). Melt drops (red colour) are shown just for illustration and are plotted in the second cell from the symmetry line (one behind the water velocity vectors). The melt volume fraction is shown where its volume fraction is larger than 0.001. Everywhere else, the water volume fraction is shown.

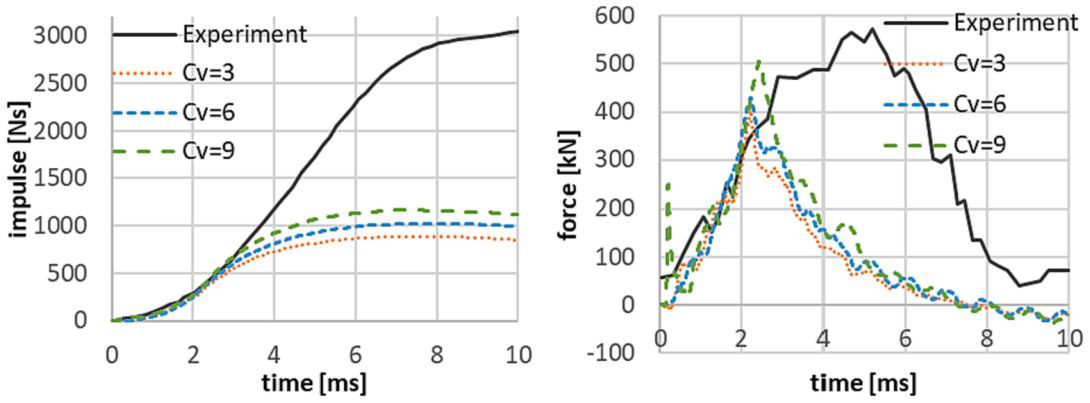

Fig. 17. Comparison of the force and total gained impulse on the bottom plate for different melt drops ejection velocity factors C_v for PULiMS E6 simulations and experiment (figure adopted from (Kokalj et al., 2021)).

ejection velocity can be modelled with the most satisfactory accuracy, relative to the other parameters. However, due to the additional phenomena of melt spreading and possible cold water ingression, the uncertainties of the initial and boundary conditions in the experiment should most probably not be neglected.

6. Conclusions with perspectives

From the perspective of nuclear safety, being able to simulate with confidence potential energetic fuel–coolant interactions in stratified configurations with the preceded premixed layer of ejected melt drops in the coolant layer is of high importance.

In the paper, a sensitivity study is performed on the previously introduced premixed layer formation model, which defines the continuous melt fragmentation rate, the size of the ejected melt drops and the ejected melt drop velocity. We use the patch of Eulerian fuel–coolant interaction code MC3D with the implemented model. The analysis is performed against the experimental results of the SES S1 and the PULiMS E6. The results are assessed mostly indirectly via the steam explosion, as the direct comparison of the premixed layer with the experimental results is limited. The previously presented base simulation results regarding the expected premixed layer height, the strength of the steam explosion and the duration of the energetic event are qualitatively and quantitatively in agreement with the experimental results. With the sensitivity study on the premixed layer formation model's main parameters, their effect on the simulation results is demonstrated.

The impact on the explosion is evident in all the conducted analyses and remains consistent in simulations for both experimental tests. Notably, the melt fragmentation rate plays a pivotal role in determining the duration of the explosion. When the fragmentation rate is higher, leading to a greater quantity of melt drops in the premixed layer, it results in a shorter vapour explosion characterized by a higher peak force. This suggests that a mixture, richer in the melt drops, enhances faster development of the explosion. The trend of producing a shorter explosion with a higher peak force is also noticeable with smaller melt drop diameters. This could be attributed to the fact that smaller melt drops undergo quicker and more rapid fine fragmentation. The fine fragmentation rate is in the code simulated to be inversely proportional to the melt drop diameter. Additionally, a significant influence of the ejection melt drop velocity on the premixed layer height but limited on the explosion strength is identified.

Comparing both experimental tests, it can be concluded that, by far, the largest effect on the overall strength of the steam explosion is the total mass of the melt in the premixed layer, i.e. the size of the melt pool and consequently of the premixed layer (in the PULiMS E6 case, the melt pool diameter was 40 cm and, in the SES S1 case, it was 25 cm). Therefore, in the reactor or other industry case, the limited area of contact between the still liquid melt pool and the coolant would predominately affect the potential risk and consequences. Among the properties of the created premixed layer that most affect the force (or pressure) peak of the possible fuel–coolant interaction are the richness of the premixed layer with melt drops and the melt drops size. The integral impulse of the explosion seems less dependent on the premixed layer properties, but less consistent results of the fragmentation rate analysis and results of the past parametric analysis implicate the need for further evaluation.

The simulation cases that closely resemble both of the examined experimental tests appear to be those where the model tuning factors C_v, C_d and C_f are set to 6, 1.25, and 0.5, respectively. The C_v value of 6 presents the best replication of the premixed layer observed in the experiments. The C_d factor 1.25 (melt drop diameter of around 8.5 mm) presents also a close match with the experimental observations. The C_f factor 0.5 is in best agreement regarding the duration of the explosion. As mentioned, the gained impulse in the simulations is underestimated, but the initial impulse gain and the force signal in the first part of these simulations are almost identical to the experimental one. After the initial increase in the force signal on the bottom, the force signal in the simulations decreases earlier compared to the experiments.

The noticed underestimation of the explosion strength in simulations possibly indicates potential additional contributions based on the other mechanisms involved in the melt-coolant mixing, formation of the premixed layer formation and following vapour explosion (e.g. jet break-up and mixing during the explosion itself). Therefore, a complete simulation of the jet pouring, fragmentation and the continuous melt spreading while simultaneously considering the premixed layer formation might gain an additional value.

Further experimental work could significantly increase our knowledge of detailed phenomena during the premixed layer formation phase in stratified configuration, also reducing the uncertainties. With the large effects of the fragmentation rate and possible other contributions on the mass of melt in the premixed layer and on the consequent vapour explosion strength, it seems most necessary to put additional effort into reducing this uncertainty. As mentioned, possible large total impulses are presenting a high risk for the systems, structures and components.

The discussed sensitivity analysis of the premixed layer formation model in the paper enables a more reliable assessment of the vapour explosions risk in nuclear power plants and other industries.

Declaration of generative AI and AI-assisted technologies in the writing process

During the preparation of this work the authors used ChatGPT language model in order to improve language and readability. After using this tool/service, the authors reviewed and edited the content as needed and take full responsibility for the content of the publication.

CRediT authorship contribution statement

Janez Kokalj: Conceptualization, Data curation, Formal analysis, Funding acquisition, Investigation, Methodology, Project administration, Software, Validation, Visualization, Writing – original draft, Writing – review & editing. **Mitja Uršič:** Conceptualization, Funding acquisition, Methodology, Software, Supervision, Writing – review & editing. **Matjaž Leskovar:** Conceptualization, Funding acquisition, Methodology, Software, Supervision, Writing – review & editing. **Renaud Meignen:** Conceptualization, Methodology, Software, Supervision, Writing – review & editing.

Declaration of competing interest

The authors declare that they have no known competing financial interests or personal relationships that could have appeared to influence the work reported in this paper.

Data availability

The authors do not have permission to share data.

Acknowledgments

The authors acknowledge the financial support from the Slovenian Research and Innovation Agency (research core funding No. P2-0026 and the projects Fuel-coolant interactions in combined stratified and melt jet configurations, Z2-4437, and Understanding stratified steam explosions in reactor conditions, L2-1828). The authors acknowledge the financial support from the state budget by the Slovenian Research and Innovation Agency (project No. V2-2375) and the Slovenian Nuclear Safety Administration. The authors acknowledge also IRSN (France) and the MC3D development team.

References

Albiol, T., Haste, T., 2008. Summary of SARNET achievements, The 3rd European Review Meeting on Severe Accident Research, ERMSAR-2008, Nesseber, Bulgaria, p. 14.

Berenson, P.J., 1961. Film-boiling heat transfer from a horizontal surface. J. Heat Transf. 83, 351–356.

Berthoud, G., 2000. Vapor explosions. Annu. Rev. Fluid Mech. 32, 573–611.

Blundell, N., 2015. OECD/SERENA Project Report: Summary and Conclusions. Report no. NEA/CSNI/R(214)15, Organisation for Economic Co-operation and Development, p. 22.

Caldarola, L., Kastenberg, W.E., 1974. Mechanism of fragmentation during molten fuel/coolant thermal interactions. In: Fast reactor safety meeting, Beverly Hills, California, USA, pp. 937-954.

Cizelj, L., Končar, B., Leskovar, M., 2006. Vulnerability of a partially flooded PWR reactor cavity to a steam explosion. Nucl. Eng. Des. 236, 1617–1627.
Corradini, M.L., Kim, B.J., Oh, M.D., 1988. Vapor explosions in light water reactors: a review of theory and modeling. Prog. Nucl. Energy 22, 1–117.
De Malmazet, E., Leskovar, M., Brayer, C., Buck, M., Buffe, L., Centrih, V., Conti, T., Haquet, J., Meignen, R., Picchi, S., 2017. Stratified Steam Explosion Phenomena: SAFEST SES-S1 test results and preliminary analysis. In: The 8th European Review Meeting on Severe Accident Research, ERMSAR-2017, Warsaw, Poland.
Gelfand, B.E., 1996. Droplet breakup phenomena in flows with velocity lag. Prog. Energy Combust. Sci. 22, 201–265.
Grishchenko, D., Konovalenko, A., Karbojian, A., Kudinova, V., Bechta, S., Kudinov, P., 2013. Insight into steam explosion in stratified melt-coolant configuration. In: 15th International Topical Meeting on Nuclear Reactor Thermal Hydraulics, Pisa, Italy, p. 19.
Haraldsson, H.Ó., Li, H.X., Yang, Z.L., Dinh, T.N., Sehgal, B.R., 2001. Effect of solidification on drop fragmentation in liquid-liquid media. Heat Mass Transf./waerme- Und Stoffuebertragung 37, 417–426.
Hong, S.-W., Piluso, P., Leskovar, M., 2013. Status of the OECD-SERENA project for the resolution of ex-vessel steam explosion risks. J. Energy Power Eng. 7, 423.
Huhtiniemi, I., Magallon, D., Hohmann, H., 1999. Results of recent KROTOS FCI tests: alumina versus corium melts. Nucl. Eng. Des. 189, 379–389.
Kokalj, J., 2021. Modelling of Fuel-Coolant Interaction in Stratified Configuration. Ph.D. thesis. University of Ljubljana, Slovenia.
Kokalj, J., Leskovar, M., Uršič, M., 2019. Premixed layer formation modelling in stratified melt-coolant geometry. In: ANS (Ed.), 18th International Topical Meeting on Nuclear Reactor Thermal Hydraulics. ANS, Portland, USA, pp. 4018-4031.
Kokalj, J., Uršič, M., Leskovar, M., 2021. Modelling of premixed layer formation in stratified fuel–coolant configuration. Nucl. Eng. Des. 378, 111261–111277.
Kokalj, J., Uršič, M., Leskovar, M., Meignen, R., 2023. Modelling and simulating of premixed layer in stratified fuel coolant configuration. Ann. Nucl. Energy 185, 109740.
Konovalenko, A., Karbojian, A., Kudinov, P., 2012. Experimental results on pouring and underwater liquid melt spreading and energetic melt-coolant interaction. In: The 9th International Topical Meeting on Nuclear Thermal-Hydraulics, Operation and Safety. American Nuclear Society, Kaohsiung, Taiwan, p. 11.
Kudinov, P., Grishchenko, D., Konovalenko, A., Karbojian, A., 2017. Premixing and steam explosion phenomena in the tests with stratified melt-coolant configuration and binary oxidic melt simulant materials. Nucl. Eng. Des. 314, 182–197.
Lamome, J., Meignen, R., 2008. On the explosivity of a molten drop submitted to a small pressure perturbation. Nucl. Eng. Des. 238, 3445–3456.
Leskovar, M., Centrih, V., Uršič, M., 2016. Simulation of steam explosion in stratified melt-coolant configuration. Nucl. Eng. Des. 296, 19–29.
Leskovar, M., Centrih, V., Uršič, M., Kokalj, J., 2019. Investigation of steam explosion duration in stratified configuration. Nucl. Eng. Des. 353, 110233.
Leskovar, M., Uršič, M., 2009. Estimation of ex-vessel steam explosion pressure loads. Nucl. Eng. Des. 239, 2444–2458.
Meignen, R., Piluso, P., Rimbert, N., 2017. Outcomes of the French ICE project on Fuel Coolant Interaction. In: 17th International Topical Meeting on Nuclear Reactor Thermal Hydraulics, Xi'an, Shaanxi, China.
Meignen, R., Picchi, S., Lamome, J., Raverdy, B., Escobar, S.C., Nicaise, G., 2014a. The challenge of modeling fuel–coolant interaction: Part I – Premixing. Nucl. Eng. Des. 280, 511–527.
Meignen, R., Raverdy, B., Buck, M., Pohlner, G., Kudinov, P., Ma, W., Brayer, C., Piluso, P., Hong, S.-W., Leskovar, M., 2014b. Status of steam explosion understanding and modelling. Ann. Nucl. Energy 74, 125–133.
Meignen, R., Raverdy, B., Picchi, S., Lamome, J., 2014c. The challenge of modeling fuel–coolant interaction: Part II – Steam explosion. Nucl. Eng. Des. 280, 528–541.
Melikhov, V.I., Melikhov, O.I., Yakush, S.E., Le, T.C., 2020. Evaluation of energy and impulse generated by superheated steam bubble collapse in subcooled water. Nucl. Eng. Des. 366, 110753.
Miassoedov, A., Journeau, C., Bechta, S., Hózer, Z., Manara, D., Bottomley, D., Kiselova, M., Langrock, G., 2015. Severe accident facilities for European safety targets. In: The SAFEST Project, 7th European Review Meeting on Severe Accident Research Conference, ERMSAR -2015, pp. 24–26.
Nelson, L.S., Duda, P.M., 1981. Steam explosion experiments with single drops of iron oxide. NUREG/CR-2285, SAND81-1672.
Nelson, L.S., Duda, P.M., 1985. Steam explosion experiments with single drops of iron oxide melted with a CO 2 laser. Part II. Parametric studies. NUREG/CR-2718, SAND82-1105.
Park, H.S., Hansson, R.C., Sehgal, B.R.J.E.t., science, f., 2005. Fine fragmentation of molten droplet in highly subcooled water due to vapor explosion observed by X-ray radiography. 29, pp. 351-361.
Pilch, M., Erdman, C.A., 1987. Use of breakup time data and velocity history data to predict the maximum size of stable fragments for acceleration-induced breakup of a liquid drop. Int. J. Multiph. Flow 13, 741–757.
Sairanen, R., Berthoud, G., Ratel, G., Meignen, R., Jacobs, H., Buerger, M., Buck, M., Moriyama, M., Naito, M., Song, J., 2007. OECD research programme on fuel-coolant interaction steam explosion resolution for nuclear applications-SERENA. Final Report-December 2006. Report no. NEA/CSNI/R(2007)11, Organisation for Economic Co-Operation and Development.
Seghal, B.R., 2012. Nuclear Safety in Light Water Reactors: Severe Accident Phenomenology. Elsevier Inc.
Theofanous, T.G., 1995. The study of steam explosions in nuclear systems. Nucl. Eng. Des. 155, 1–26.
Turland, B.D., Dobson, G.P., 1996. Molten fuel coolant interactions: A state of the art report. Report no. European Commission Report 16874, AEA.
Uršič, M., Leskovar, M., 2010. Analysis of ex-vessel steam explosion pressure loads. Strojniski Vestnik/J. Mech. Eng. 56.
Uršič, M., Leskovar, M., Mavko, B., 2011. Improved solidification influence modelling for Eulerian fuel–coolant interaction codes. Nucl. Eng. Des. 241, 1206–1216.
Yakush, S.E., Sivakov, N.S., 2023. Numerical modeling of high-temperature melt droplet interaction with water. Ann. Nucl. Energy 185, 109718.